Advances in Science and Technology Vol. 74 (2010) pp 196-204

doi:10.4028/www.scientific.net/AST.74.196

Optical Methods for Indoor Characterization of Small-Size Solar Concentrators Prototypes

Antonio Parretta[1,2a]*, Andrea Antonini [3,b], M.A. Butturi[3,c], E. Milan[3,d], Pierangelo Di Benedetto[3,e], Davide Uderzo[3,f], Paolo Zurru[3,g]

[1]ENEA, Centro Ricerche "E. Clementel", Via Martiri di M.te Sole, 40129 Bologna, Italy

[2]Università di Ferrara, Dipartimento di Fisica, Via Saragat, 1, 44122 Ferrara, Italy

[3]CPower SRL, Via Ferrari 31/d, 44122 Ferrara (FE), Italy

[a]parretta@fe.infn.it, [b]andrea.antonini@cpower.it, [c]mariangela.butturi@cpower.it, [d]emiliano.milan@cpower.it, [e]pierangelo.dibenedetto@cpower.it, [f]davide.uderzo@cpower.it, [g]paolo.zurru@cpower.it

Keywords: Nonimaging concentrators; characterization; transmission efficiency; direct irradiation; inverse irradiation.

Abstract. The light collection properties of different types of solar concentrators have been investigated by applying conventional and innovative methods of characterization [1, 2]. Four types of optical methods were applied: i) a "direct" method using a laser beam as light source; ii) a "direct" method using a parallel beam simulating the direct component of solar light; iii) a "direct" integral method using a lambertian light source simulating the diffuse component of solar light; iv) an "inverse" method using a lambertian light source applied at the receiver side, thereby reversing the light path. The optical properties derived by applying the above three methods were: i) the local optical collection efficiency, resolved on the entrance point and direction of incidence ii) the overall optical collection efficiency under collimated light, resolved on direction of incidence; iii) the spatial and angular distribution of flux on the receiver.

Introduction

Several methods can be applied to the optical characterization of solar concentrators. In this paper we focus our attention to the two classes directly derived by our research on this subject: "direct" and "inverse", distinguishing the way the concentrator is irradiated, if from the input or the output aperture, respectively. In this sense, the term "direct" is by no means to be associated to the direct component of solar radiation. To test the concentrator, we will consider, for example, the direct "local" irradiation, by using a laser light, or the direct "collimated" irradiation, by using a plane wave simulating the direct component of solar light, or finally the direct "integral" irradiation, by using a lambertian light representing the diffuse component of solar light. The "inverse" method will be applied only by using a lambertian light source.
We investigate mainly concentrators derived by the nonimaging optics, like the well known Compound Parabolic Concentrators (CPC) [1, 2], with ideal or modified shape, to reduce its length or to optimize its packing in a module [3].

The methods of characterization

The "direct local method". The *"direct local method"*, or *"laser method"* (DLM) is the simplest method of characterization to be applied. It uses a laser beam to scan the input aperture following a matrix of points at fixed orientation direction (polar and azimuthal angles θ and φ) [4]. The flux

measured at output aperture allows to draw a map of "local" transmission efficiency, that can be compared to the map derived by raytracing the CAD model of concentrator, giving in such a way information about local surface/interface defects or manufacturing inaccuracies of the substrate. Fig. 1a shows the schematic experimental setup of DLM method.

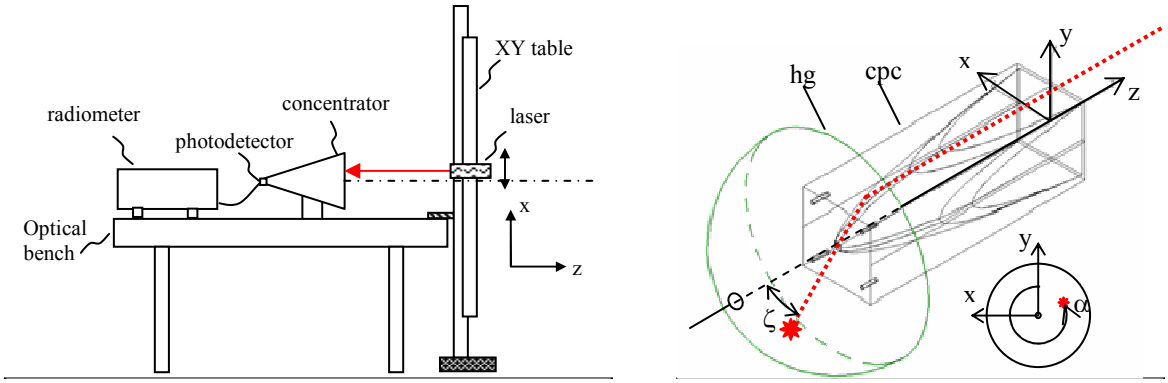

a) b)

Figure 1. Experimental set-up of the laser characterization of 3D-CPC concentrators. Measure of output flux (a); measure of output beam divergence (b).

The measure of exit angles of laser beam at output aperture of concentrator can be carried out by using the simple apparatus of Fig. 1b. A plastic hemispherical globe (hg) is centered on the output aperture of the CPC and drawn with parallels and meridians representing the polar and azimuthal angles of the laser beam spot. The opalescence of the globe allows to visualize the impact point of the laser beam and then, with a good approximation, its exiting direction.

The "direct collimated method". The angle-resolved transmission efficiency of the whole concentrator is obtained irradiating the entire input aperture by a suitably oriented parallel beam and measuring the output flux (*"direct collimated method"* or DCM) (Fig. 2a). From the transmission curve we derive the acceptance angle, θ_{acc}, conventionally the angle at 50% of the 0° efficiency (90% for photovoltaic applications) (Fig. 2b). Besides the "absolute" optical efficiency $\eta(\theta,\varphi)$, it is useful to consider the efficiency normalized to 0° value: $\eta_{rel}(\theta,\varphi) = \eta(\theta,\varphi)/\eta(0)$. As we will see in the following, the normalized efficiency curve can be obtained in a very simple way by applying the *"inverse"* method. Fig. 2c shows the DCM apparatus during characterization of "Rondine" nonimaging concentrator [5]. The beam from the integrating sphere (is1) is collimated by the parabolic mirror (pm1) and irradiates the concentrator (cpc). The output flux, measured by the integrating sphere (is2) at different orientations of the (cpc), gives the relative transmission efficiency $\eta_{rel}(\theta,\varphi)$. A separate measure on the input beam gives the input flux and allows to calculate the absolute transmission efficiency $\eta(\theta,\varphi)$.

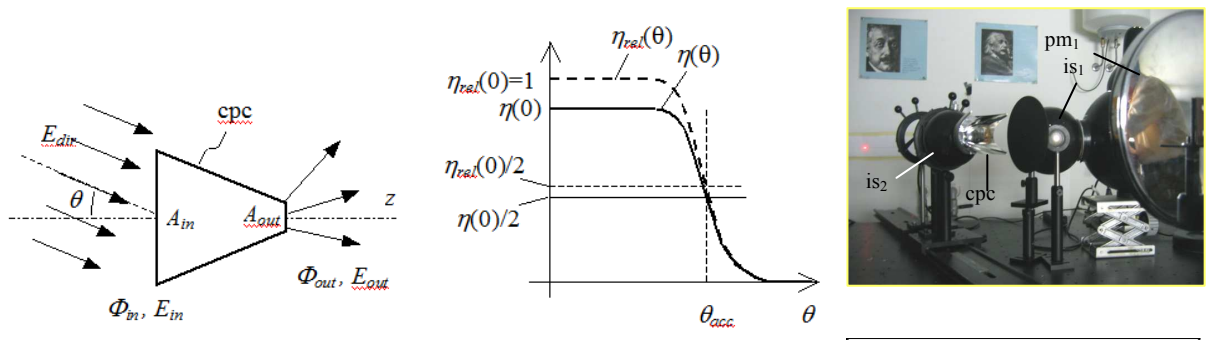

a) b) c)

Figure 2. Scheme of the DCM method (a). Absolute and relative transmission curves of a typical 3D-CPC concentrator (b). Photo of the DCM apparatus (c).

The "direct integral method". The *"direct integral method"* (DIM) has been introduced to study the transmission efficiency of a concentrator integrated over all the directions at input. DIM simulates the behaviour of the concentrator under the diffuse component of solar radiation, when it is uniform. Fig. 3a shows the scheme of DIM applied to a 3D-CPC concentrator, with L_{dir} constant radiance of the diffused light source. The DIM can be realized in practice using a suitably illuminated hemispherical, lambertian screen (s) of radius $R>>\sqrt{A_{in}}$. DIM gives the *"direct integral transmission efficiency"* η_{dir}^{int}, defined as the ratio of output to input flux:

$$\eta_{dir}^{\text{int}} = \frac{\Phi_{dir}^{\tau}}{\Phi_{dir}^{in}} = \frac{1}{\pi} \cdot \int_0^{2\pi} d\varphi \int_0^{\pi/2} d\theta \cdot \sin\theta \cdot \cos\theta \cdot \eta_{dir}(\theta,\varphi) = \frac{1}{\pi} \cdot \eta_{dir}(0) \cdot \int_0^{2\pi} d\varphi \int_0^{\pi/2} d\theta \cdot \sin\theta \cdot \cos\theta \cdot \eta_{dir}^{rel}(\theta,\varphi). \quad (1')$$

$$\eta_{dir}^{\text{int}} = \frac{\Phi_{dir}^{\tau}}{\Phi_{dir}^{in}} = 2 \cdot \int_0^{\pi/2} d\theta \cdot \sin\theta \cdot \cos\theta \cdot \eta_{dir}(\theta) = 2 \cdot \eta_{dir}(0) \cdot \int_0^{\pi/2} d\theta \cdot \sin\theta \cdot \cos\theta \cdot \eta_{dir}^{rel}(\theta). \quad (1'')$$

where Eq. (1') applies to a generic concentrator and Eq. (1'') to a cylindrical concentrator, and the symbol "τ" means *transmitted*. In a similar way we can define the other two quantities related to DIM: the *"direct integral absorptance"* $\alpha_{dir}^{\text{int}}$ and the *"direct integral reflectance"* ρ_{dir}^{int} (hereafter we limit to cylindrical symmetry for simplicity):

$$\alpha_{dir}^{\text{int}} = \frac{\Phi_{dir}^{\alpha}}{\Phi_{dir}^{in}} = 2 \cdot \int_0^{\pi/2} d\theta \cdot \sin\theta \cdot \cos\theta \cdot \alpha_{dir}(\theta) = 2 \cdot \alpha_{dir}(0) \cdot \int_0^{\pi/2} d\theta \cdot \sin\theta \cdot \cos\theta \cdot \alpha_{dir}^{rel}(\theta). \quad (2)$$

$$\rho_{dir}^{\text{int}} = \frac{\Phi_{dir}^{\rho}}{\Phi_{dir}^{in}} = 2 \cdot \int_0^{\pi/2} d\theta \cdot \sin\theta \cdot \cos\theta \cdot \rho_{dir}(\theta) = 2 \cdot \rho_{dir}(0) \cdot \int_0^{\pi/2} d\theta \cdot \sin\theta \cdot \cos\theta \cdot \rho_{dir}^{rel}(\theta). \quad (3)$$

where: $\eta_{dir}^{\text{int}} + \alpha_{dir}^{\text{int}} + \rho_{dir}^{\text{int}} = 1$.

The average output radiance is expressed as:

$$\overline{L}_{dir}^{out} = \frac{\Phi_{dir}^{\tau}}{\pi \cdot A_{out}} = \frac{2 \cdot L_{dir} \cdot A_{in}}{A_{out}} \cdot \int_0^{\pi/2} d\theta \cdot \sin\theta \cdot \cos\theta \cdot \eta_{dir}(\theta) = 2 \cdot L_{dir} \cdot C_{geo} \cdot \int_0^{\pi/2} d\theta \cdot \sin\theta \cdot \cos\theta \cdot \eta_{dir}(\theta) \quad (4)$$

Now we define the quantity $\lambda_{dir(\alpha)}$ as the ratio between output and input radiance:

$$\lambda_{dir} = \frac{\overline{L}_{dir}^{out}}{L_{dir}} = 2 \cdot C_{geo} \cdot \int_0^{\pi/2} d\theta \cdot \sin\theta \cdot \cos\theta \cdot \eta_{dir}(\theta) = 2 \cdot C_{geo} \cdot \int_0^{\pi/2} d\theta \cdot \sin\theta \cdot \cos\theta \cdot [1 - \alpha(\theta) - \rho(\theta)] \quad (5)$$

From the previous equations we find the relationship:

$$\lambda_{dir} = \frac{\overline{L}_{dir}^{out}}{L_{dir}} = \eta_{dir}^{\text{int}} \cdot C_{geo} = \frac{\Phi_{dir}^{\tau}}{\Phi_{dir}^{in}} \cdot \frac{A_{in}}{A_{out}} = \frac{\overline{E}_{out} \cdot A_{out}}{E_{in} \cdot A_{in}} \cdot \frac{A_{in}}{A_{out}} = \frac{\overline{E}_{out}}{E_{in}} \quad (6)$$

similar to the relationship defining the optical concentration ratio under collimated beam irradiation:

$$C_{opt} = \frac{E_{out}}{E_{in}} = \eta_{dir} \cdot C_{geo} = \frac{\Phi_{out}}{\Phi_{in}} \cdot \frac{A_{in}}{A_{out}} \quad (7)$$

We can define therefore the quantity λ_{dir} as the "*optical concentration ratio under direct integral irradiation*" or "*direct integral concentration ratio*". From Eq. (6) we see that λ_{dir} can be expressed also as the ratio between the average output and input irradiances.
Fig. 3(a) shows the schematic principle of DIM. For small size concentrators, the DIM can be carried out indoors by using an integrating sphere to produce a uniform lambertian irradiation over the input aperture (see Fig. 3b). Input and output fluxes can be then measured by alternating a photodetector (pd) on the input and output apertures. The DIM can be carried out also outdoors by simply exposing the concentrator to the diffuse component of solar radiation, after removing the direct component by a shadow band (sb) (see Fig. 3c). To get new interesting information about properties of a CPC, the DIM can be applied by changing the angular aperture of the lambertian source (see Results).

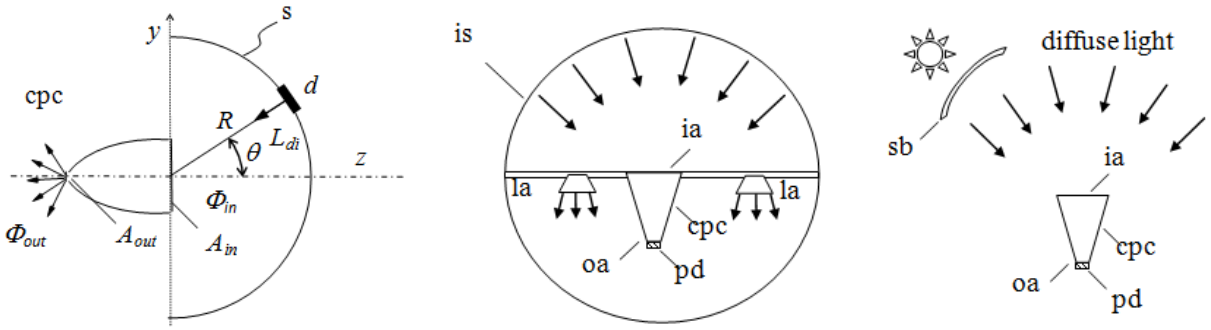

a) b) c)

Figure 3. Scheme of the DIM method (a). Indoor application of DIM by using an integrating sphere (b). Outdoor application of DIM by using the diffused solar light (c).

The "inverse method". With the "*inverse method*" (IM) we test the concentrator by irradiating the output aperture, therefore reversing the light path occurring during normal operation. The inverse method [6, 7] is an alternative way to obtain the angle-resolved optical efficiency of a concentrator. It is characterized by a remarkable rapidity of measurements and by a simple apparatus with respect to direct methods (DM). The "conventional" IM is applied by irradiating the overall output aperture by a *lambertian* source (ls) (Fig. 4a). Light projected from the input aperture (ia) over the screen (sc) (Fig. 4b) produces an irradiance distribution $E_{inv}^{rel}(\theta,\varphi)$ whose profile, corrected by the $\cos^{-4}(\tau)$ factor, gives the relative radiance $L_{inv}^{rel}(\theta,\varphi)$ of concentrator towards (θ,φ) direction. It can be demonstrated [6, 7] that $L_{inv}^{rel}(\theta,\varphi)$ is equivalent to the relative "direct" angle-resolved transmission efficiency $\eta_{dir}^{rel}(\theta,\varphi)$ obtained by the collimated direct method (DCM): $L_{inv}^{rel}(\theta,\varphi)=\eta_{dir}^{rel}(\theta,\varphi)$. The measure of $E_{inv}^{rel}(\theta,\varphi)$ is done by CCD recording of the image on the screen (sc). The correctness of equality: $L_{inv}^{rel}(\theta,\varphi)=\eta_{dir}^{rel}(\theta,\varphi)$ has been widely demonstrated by us by optical simulations of both DM and IM for several types of concentrators, both reflective and refractive (see Results). The IM so far described gives the relative optical efficiency of concentrator, $\eta_{dir}^{rel}(\theta,\varphi)$. To have the absolute optical efficiency, $\eta_{dir}(\theta,\varphi)=\eta_{dir}^{rel}(\theta,\varphi)\cdot\eta_{dir}(0)$, we need to measure $\eta_{dir}(0)$. This can be done by applying the IM in a different way, that is by orienting the CCD camera towards the concentrator input aperture and measuring its radiance (Fig. 5a). It can be demonstrated that $\eta_{dir}(0)$ is given by the ratio $\overline{L}_C(0)/L_{RIC}$, where $\overline{L}_C(0)$ is the average radiance of the whole input aperture and L_{RIC} is the radiance of the receiver, that is of the lambertian source (ls) [8]. Fig. 5b shows an example of measure of $\eta_{dir}(0)$: $\overline{L}_C(0)$ is the average radiance inside the big red circle, L_{RIC} is the average radiance inside the small blue circle.

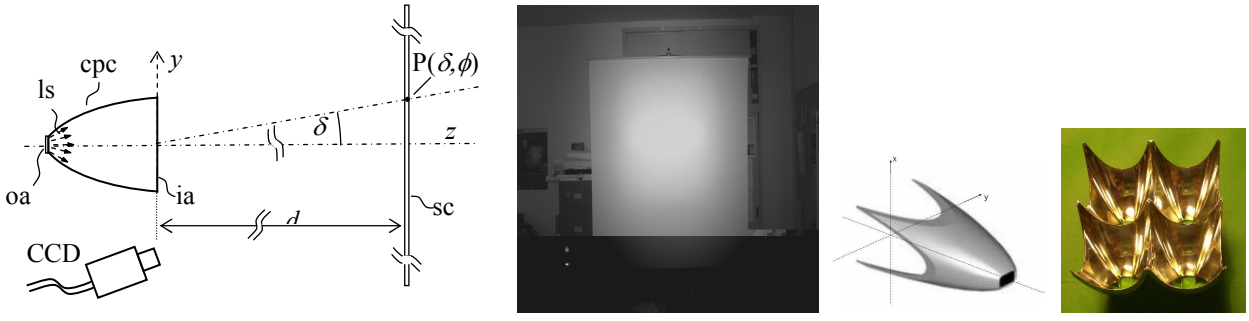

a) b) c)

Figure 4. a) Schematic principle of IM. b) Image produced on the screen (sc). c) "Rondine" concentrator (old and new version respectively).

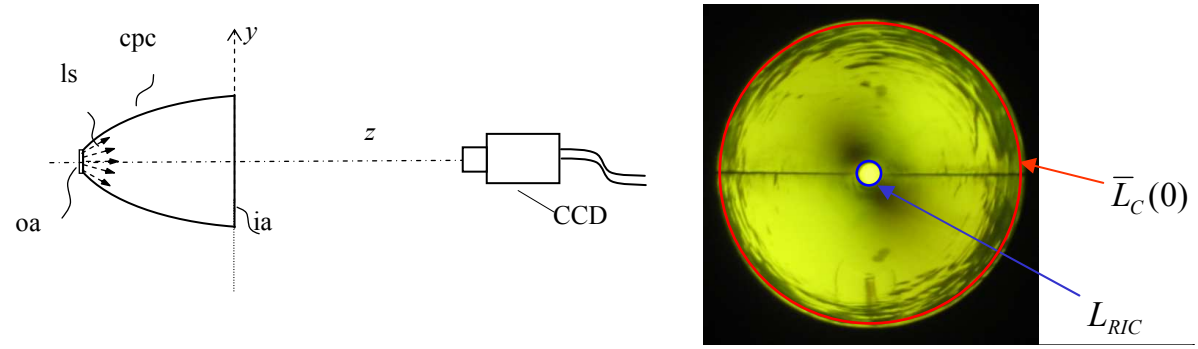

a) b)

Figure 5. a) Schematic principle of IM applied to the evaluation of $\eta_{dir}(0)$ through the measure of radiance of input aperture of the CPC (a). Measure of inverse radiance of a truncated CPC (b).

The IM can be applied also locally, by irradiating only a portion of output aperture by a *lambertian* source, therefore becoming a *"local inverse method"* (LIM) [6]. In this way LIM explores the *direct* transmission efficiency of specific regions of receiver, allowing to establish which directions are more effective for their optical collection in *direct* mode. A final remark about the correct application of IM is of extreme importance: light from the inverse lambertian source must be *unpolarized*. The best way to achieve this is to use an integrating sphere. An alternative, but less practical, method is the use of a high reflectivity lambertian diffuser illuminated by the front side of concentrator. Another alternative, but less effective, method is the use of a semitransparent diffuser illuminated by the back side of concentrator; in this case it is more difficult to obtain a good lambertian distribution of transmitted light.

Results

Examples of experimental and simulated maps of "local" transmission efficiency for a CPC with square-shaped input aperture and reflective walls realized by strips of 3M VM2000 radiant mirror films are reported in Figs. 6a,b. From the map of local efficiency it is derived the average transmission efficiency for a particular incidence angle. Different maps allow to draw the transmission efficiency curve (see Fig. 6c). Maps of exit angles of laser beam for the square-shaped CPC are reported in Fig. 7. The maps show a well defined symmetry. The polar angle map (a) shows that rays incident on the periphery of input aperture (ia) exit from the CPC with a small divergence. The divergence increases at decreasing the distance between impact point and center of (ia). The central region of polar map is rather confused. Here the beam spot on the screen (hg) is very dispersed and so impossible to measure. Fig. 7b shows that the azimuth angle also varies very regularly with the coordinate of input beam. At an entrance point on (ia) corresponds an exit direction opposite with respect to the centre of aperture. Then, if we let the input ray move on a circle

clockwise around the centre, the exiting azimuth will regularly increase and the polar angle will remain constant. At the centre of the map we note the same irregularities as for the polar angle map.

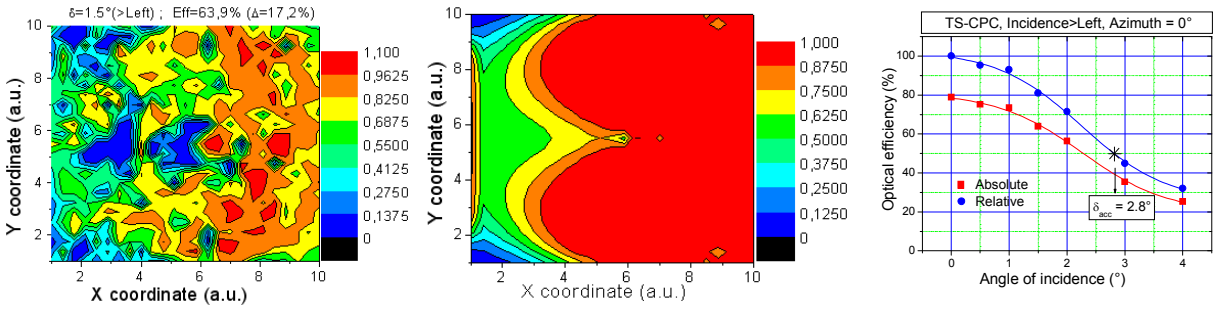

a) b) c)

Figure 6. Example of the experimental DLM map obtained at 1.5° incidence of laser beam for a CPC with square-shaped input aperture [4] (a). The same map as obtained simulating the DLM by an optical code on the CAD model (b). The absolute and relative transmission curves obtained by averaging the experimental maps (a) at different incidence angles (c).

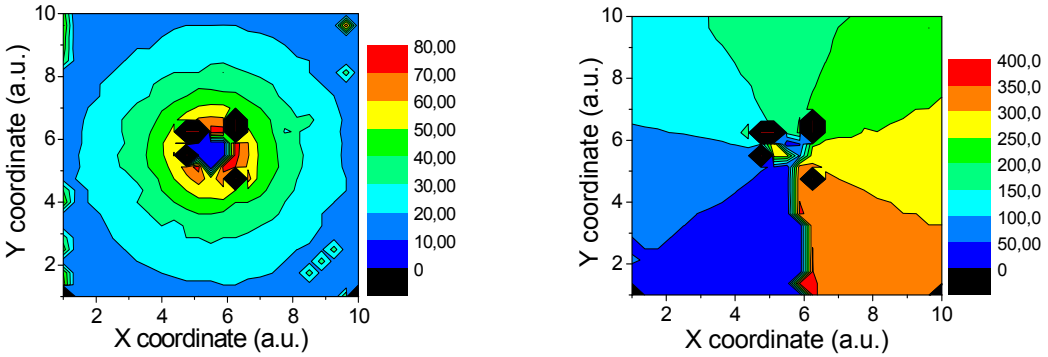

a) b)

Figure 7. Input aperture maps of polar (a) and azimuthal (b) angles of the laser beam exiting from the output aperture of the square-shaped CPC, at $\theta = 0°$ polar incidence angle at input.

The validity of equivalence $L_{inv}^{rel}(\theta,\varphi) = \eta_{dir}^{rel}(\theta,\varphi)$ has been widely demonstrated by us by optical simulations of both DCM and IM methods for several types of concentrators. The simulated angle-resolved transmission efficiency curves of two types of concentrators, a truncated 3D-CPC and a circular Fresnel lens, are shown in Fig. 8. They have been obtained by applying both DCM and IM methods, which give the same results, as can be seen by the perfect overlapping of the corresponding curves.

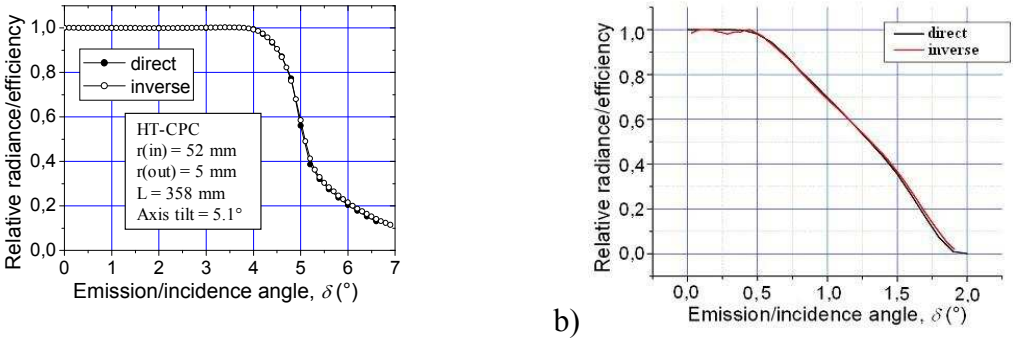

a) b)

Figure 8. Comparison between *"relative inverse radiance"* and *"relative direct transmission efficiency"* obtained by IM and DCM simulations for: a) a half-truncated CPC with 5.1° acceptance angle, b) a circular Fresnel lens.

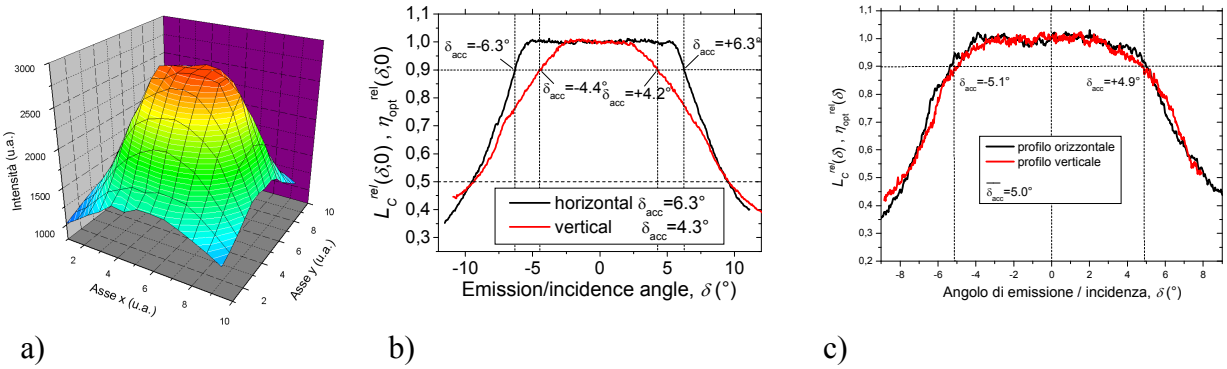

a) b) c)

Figure 9. Intensity map of the CCD image of "Rondine" concentrator (old version) (a). Horizontal and vertical profiles of inverse radiance for the old (b) and new (c) version of Rondine concentrator.

Some IM experimental results applied to "Rondine" concentrator (see Fig. 4c) are shown in Fig. 9. Fig. 9a shows the intensity distribution of the recorded image on the screen (sc). After elaboration of this image, we obtain the inverse radiance (direct transmission efficiency) profiles along horizontal and vertical directions as shown in Fig. 6b, and the corresponding (photovoltaic) acceptance angles: θ_{acc}= 6.3° (horizontal); θ_{acc}= 4.3° (vertical). The new version of Rondine concentrator (see Fig. 4c), smaller in dimension and with a square shaped output aperture, has been also characterized. The inverse radiance (direct transmission efficiency) profiles along horizontal and vertical directions of this concentrator are reported in Fig. 9c, and the corresponding (photovoltaic) acceptance angles are: θ_{acc}= 5.0° for both horizontal and vertical directions.

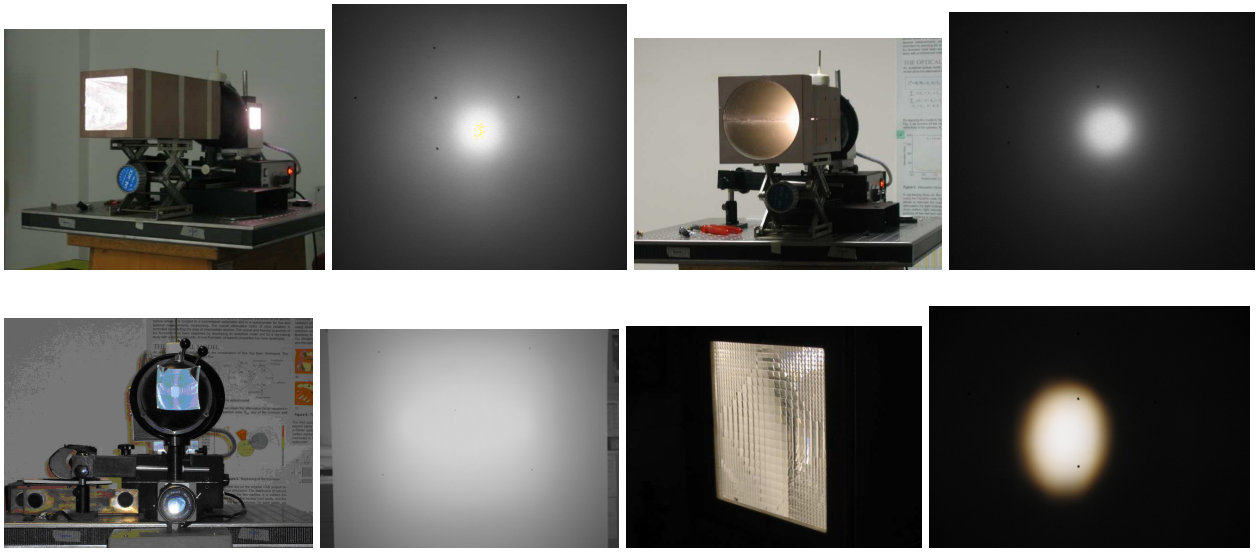

Figure 10. Photo of input aperture, irradiated in the inverse way, and the corresponding image on the screen, of some tested concentrators. Square-shaped 3D-CPC (up left). Truncated 3D-CPC (up right). Rondine (old version) (down left). Prismatic-lens PhoCUS concentrator (down right).

Some photos of concentrators irradiated in the inverse way are shown in Fig. 10, together with the corresponding inverse image produced on the screen (sc).
The application of DIM method gives very useful information when it is simulated. It has allowed to demonstrate for example that, for an ideal CPC concentrator ($\alpha_{dir}(\theta,\varphi)=0$), the output flux is uniform on the receiver plane (see Fig. 11a), whereas, for an absorbing CPC concentrator ($\alpha_{dir}(\theta,\varphi)\neq 0$), the output rays at the rim of receiver are more attenuated (see Fig. 11b). From this we argue that rays performing more reflections are preferentially directed towards the periphery of receiver. By analyzing the angular distribution of output flux (this method requires the opening of output aperture

and the application of a hemispherical absorbing screen in front of it), we find also that, with a non absorbing wall CPC we obtain a lambertian distribution of flux at output (constant output radiance L_{dir}^{out}). In presence of absorption, on the contrary, the output flux is no more lambertian. In this case we get an average radiance at output, $\overline{L}_{dir}^{out}$, always lower than L_{dir}^{out}. By the same analysis, we find also that, with an absorbing wall concentrator, the more diverging rays at output are more attenuated, further arguing therefore that rays exiting near the rim of receiver are more divergent. The above simulations becomes very useful for studying the behaviour of concentrator when they are carried out at different values of maximum divergence of the *lambertian* light at input. Fig. 11c shows for example that, for an angular aperture of lambertian source, θ_{max}=4°, smaller than the acceptance angle θ_{acc}=5°, we obtain a relative decrease of flux distribution at the rim of receiver, demonstrating that more divergent input rays are collected on the periphery of receiver.

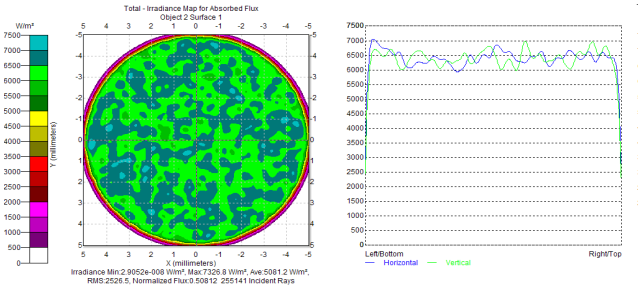

a)

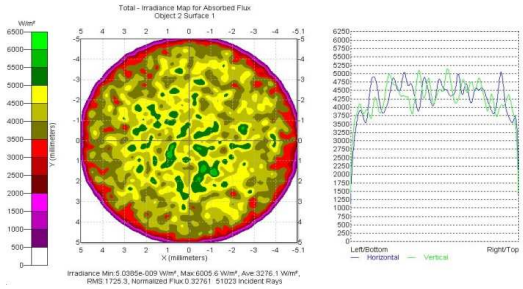

b)

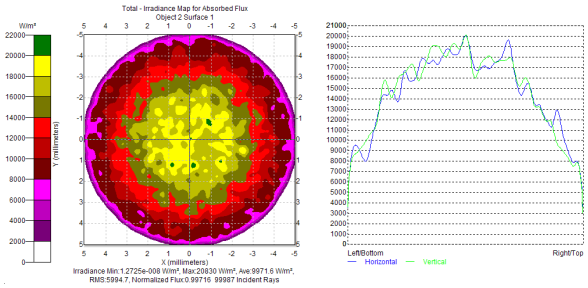

c)

Figure 11. Simulated flux distribution and x/y profiles at the output of a CPC concentrator (θ_{acc}=5°, C_{geo}=132). Ideal concentrator with wall reflectance R_w=1.0, θ_{max}=7° (a). Real concentrator with wall reflectance R_w=0.8, θ_{max}=7° (b). Ideal concentrator with wall reflectance R_w=1.0, θ_{max}=4° (c).

Summary

We have explored two classes of methods of characterization of solar concentrators, mainly of the nonimaging type: *"direct"* and *"inverse"*, in relation to the way they are irradiated, if from the input or from the output aperture. We have investigated the optical collection efficiency under collimated and diffused light.

References

[1] R. Winston, J.C. Miñano, P. Benítez, "*Nonimaging Optics*", Elsevier Academic Press, 2005.

[2] J. Chaves, "*Introduction to Nonimaging Optics*", CRC Press, 2008.

[3] A. Parretta, P. Morvillo, C. Privato, G. Martinelli, R. Winston, "*Modelling of 3D-CPCs for concentrating photovoltaic systems*", in PV in Europe, from PV Technology to Energy Solutions, Rome, Italy, 7-11 Oct. 2002 (WIP-Munich and ETA-Florence, 2002), pp.547-550.

[4] A. Parretta, A. Antonini, M. Stefancich, V. Franceschini, G. Martinelli, M. Armani, "*Characterization of CPC solar concentrators by a laser method*", in Optical Modeling and

Measurements for Solar Energy Systems, ed. by Daryl R. Myers, Proc. SPIE Vol. 6652, pp. 665207 1-12.

[5] A. Antonini, M.A. Butturi, P. Di Benedetto, D. Uderzo, P. Zurru, E. Milan, M. Stefancich, M. Armani, A. Parretta, N. Baggio, "*Rondine® PV Concentrators: Field Results and Developments*", Progress in Photovoltaics **17,** 451-459 (2009).

[6] A. Parretta, A. Antonini, M. Stefancich, G. Martinelli, M. Armani, "*Inverse illumination method for characterization of CPC concentrators*", in Optical Modeling and Measurements for Solar Energy Systems, ed. by Daryl R. Myers, Proc. of SPIE Vol. **6652**, pp. 665205 1-12.

[7] A. Parretta, A. Antonini, E. Milan, M. Stefancich, G. Martinelli, M. Armani, "*Optical efficiency of solar concentrators by a reverse optical path method*", Optics Letters **33**, 2044-2046 (2009).

[8] A. Parretta, A. Antonini, E. Bonfiglioli, M. Campa, D. Vincenzi, G. Martinelli, "*Il metodo inverso svela le proprietà dei concentratori solari*", PV Technology, n. 3, Agosto/Settembre 2009, pag. 58-64.